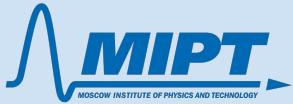




Russian Science  
Foundation

This study has been  
supported by the Russian  
Science Foundation grant  
20-72-10078



# The zoo of brightness temperature distribution in parsec-scale AGN jets

Evgeniya Kravchenko & Ilya Pashchenko  
Moscow Institute of Physics and Technology  
Astro Space Center of Lebedev Physical Institute

Based on Kravchenko et al. in prep.

# Tb along the jet. Observations and analysis

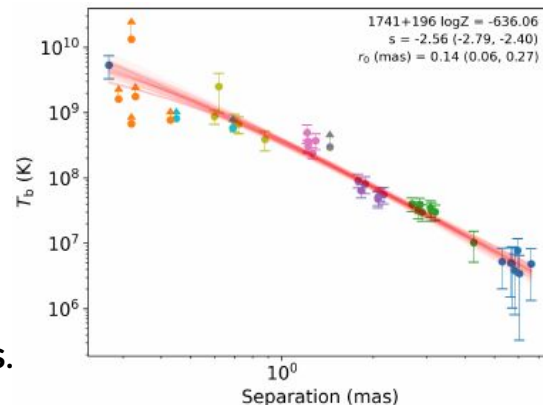
High brightness temperatures ( $T_b$ ) observed in the AGN jet radio cores (e.g. [Kovalev+2016](#), [Kravchenko+2020](#)).

When a blob of relativistic plasma propagates downstream the outflow, it loses energy through synchrotron and adiabatic mechanisms, expanding in size. These factors lead to the rapid, power-law decrease in  $T_b$  along the jet (e.g. [Lobanov&Zensus 1999](#)):  $R \sim r^d$ ;  $T_b \sim r^s$ ;  $T_b \sim R^{s'}$  ([Kadler et al. 2004](#); [Kadler PhDT 2005](#); [O'Sullivan et al. 2011](#)).

In this work, we considered the sample of **448** AGN jets observed within the MOJAVE at 15 GHz between 1994 and 2019.

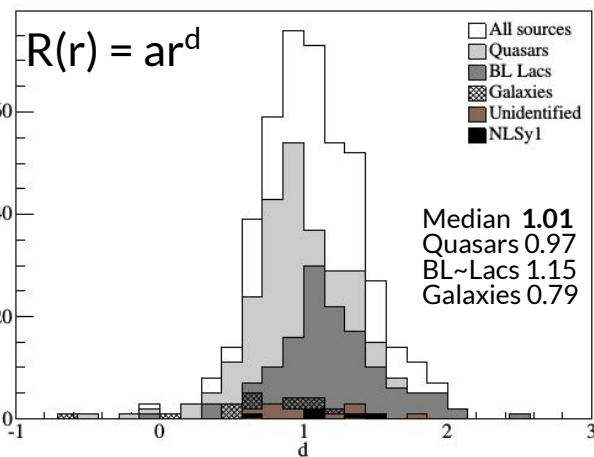
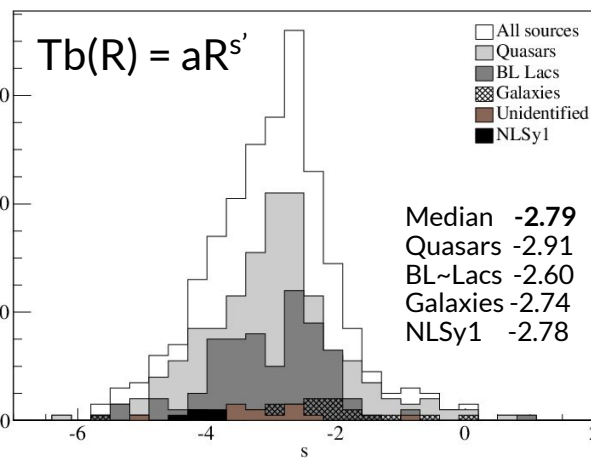
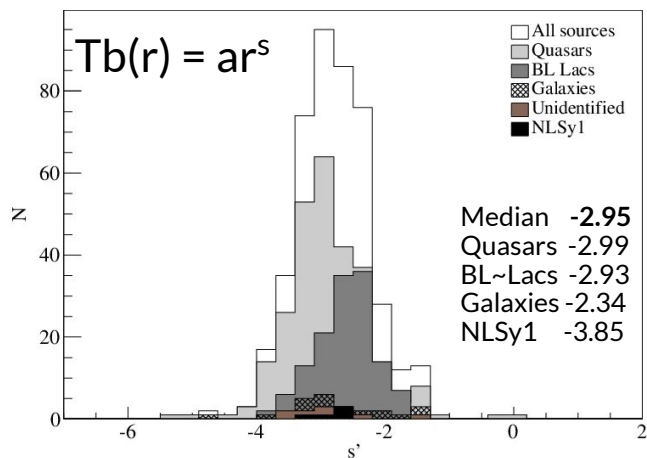
271 quasars, 141 blazars, 25 galaxies, 5 NLSy1s, 6 unidentified.

The jet structure was modelled using 2D Gaussians by a set of **components**.



Only jet **components**. Analysis of the core properties is given in [Kovalev+2005](#), [Homan+2006](#), [Kovalev+2009](#).

# Results for the single power-laws



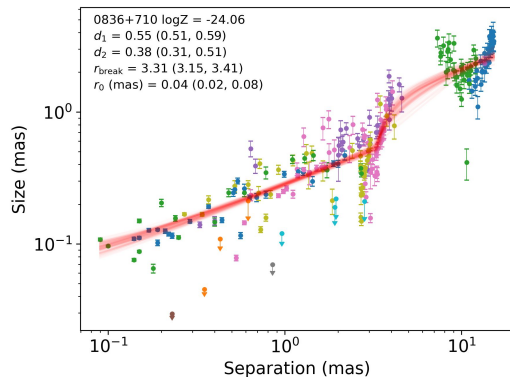
Comparison with [Pushkarev+2012;2017;Kovalev+2020](#):

median  $d = -2.2$  (2-8 GHz)

median  $d = -2.7$  (2-8 GHz)

The jets are mostly conical

median  $d = 1.02$  (15 GHz)



Components are the good tracer of jet geometry!

Distance to the true jet apex ( $r_0$ ) from the 15 GHz radio core:  $R(r) = a_1(r+r_0)^{d_1}$

Difference in our estimates of  $r_0$  and core-shifts estimates by [Pushkarev+2012](#) (8-15 GHz, 163 jets): our median = **0.118 mas**, core shift median = **0.128 mas**.

If we combined these and estimate geometry of the flow in the core region, then  $r_c \sim v^{0.84}$ . I.e. radio cores lie in the parabolically expanding region!

# Fit with a break

We observed many complex profiles, which were fitted by double power-law (broken) models:

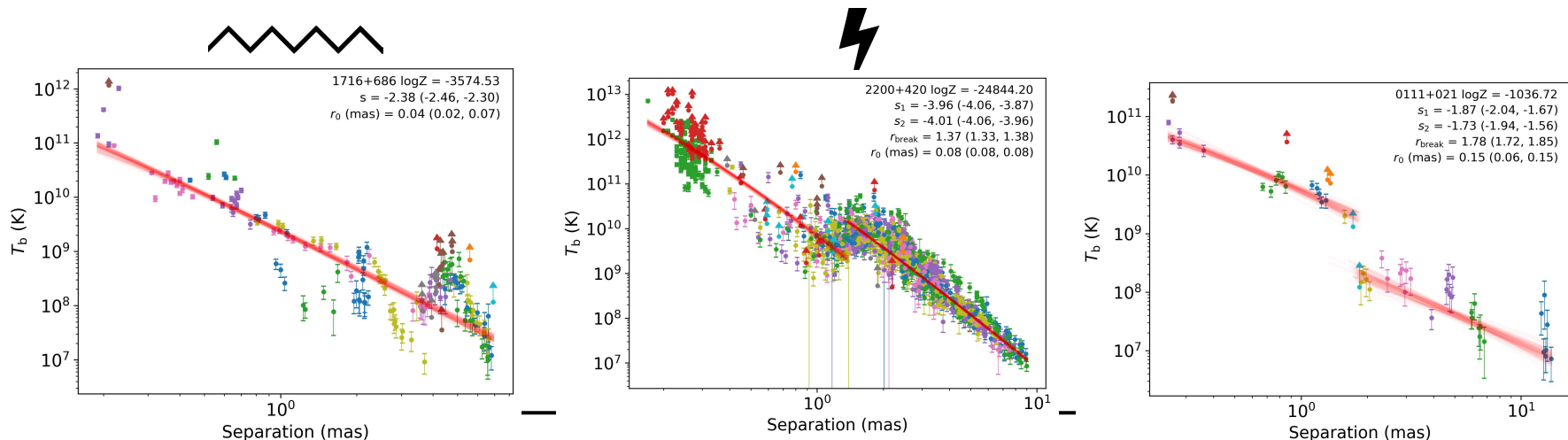
$$R(r) / T_b(r) / T_b(R) = a_1(r+r_0)^{d_1}, \text{ if } r < r_{\text{break}}$$

$$a_2(r+r_1)^{d_2}, \text{ if } r > r_{\text{break}}$$

Bayes factor for a model selection (a ratio of the marginal likelihoods of two competing models).

Detected number of significant breaks: 135 (30%) in  $T_b(r)$  / 141 (31%) in  $T_b(R)$  / 78 (17%) in  $R(r)$ .

There are mainly two types of profiles: multiple “zigzag” or “lighting” patterns and breaks.



# Change in collimation profiles

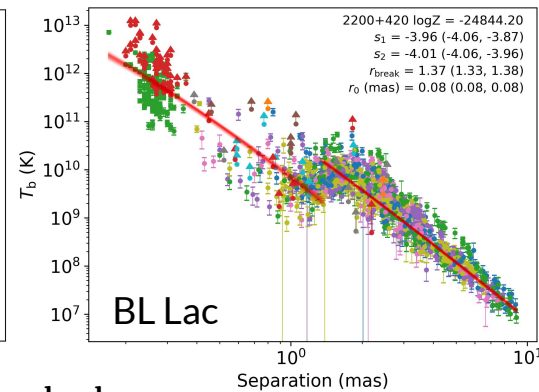
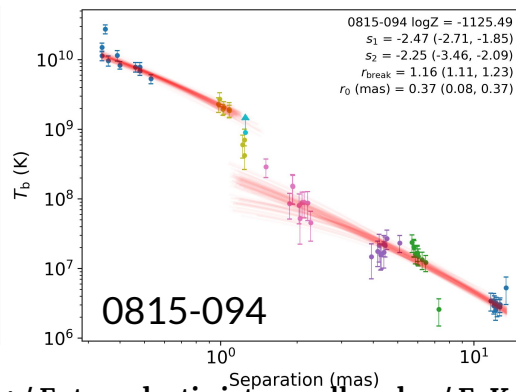
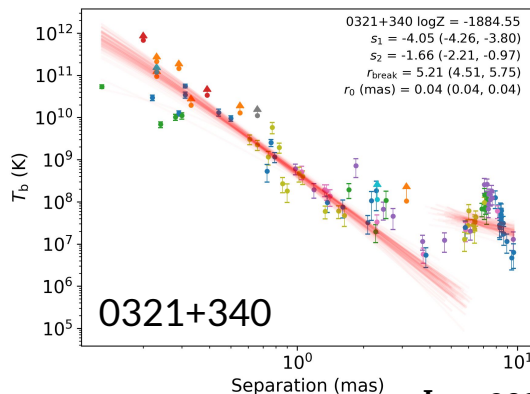
Source	Name	Opt ID	Redshift	$r_{b,R}$ (mas)	$r_{b,T}$ (mas)	$r_{b,Litr.}$ (mas)	Reference
(1)	(2)	(3)	(4)	(5)	(6)	(7)	(8)
0055+300	NGC 315	G	0.0165	$\sim 3$	$\sim 3$	$\sim 20$	Boccardi et al. (2020), Park et al. (2020)
0111+021	UGC 00773	B	0.047	$3.3^1$	$1.8 \pm 0.1$	$2.5 \pm 0.3$	Kovalev et al. (2020)
0238-084	NGC 1052	G	0.005	$3.1^1$	$2.9^1$	$2.9 \pm 0.6$	Kadler et al. (2004); Kovalev et al. (2020)
0321+340	1H 0323+342	N	0.061	$\sim 8^2$	$5.2 \pm 0.6$	7	Hada et al. (2018)
0415+379	3C 111	G	0.049	$7.5 \pm 0.4$	$4.18 \pm 0.02$	$7.0 \pm 0.5$	Kovalev et al. (2020)
0430+052	3C 120	G	0.033	$\sim 18.6$	-	$2.7 \pm 0.4$	Kovalev et al. (2020)
0815-094	TXS 0815-094	B	...	$1.3 \pm 0.1$	$1.16 \pm 0.06$	$1.4 \pm 0.3$	Kovalev et al. (2020)
1133+704	Mrk 180	B	0.045	$\sim 1^2$	$\sim 1^1$	$1.39 \pm 0.09$	Kovalev et al. (2020)
1142+198	3C 264	G	0.02172	$1.7 \pm 0.3$	$3.5 \pm 0.4$	$\sim 4$	Boccardi et al. (2019)
1226+023	3C 273	Q	0.158	$4.95 \pm 0.14$	-	$\sim 4$	Akiyama et al. (2018)
1514+004	PKS 1514+00	G	0.052	$5.1 \pm 0.4$	$\sim 1.1^1$	$3.1 \pm 0.2$	Kovalev et al. (2020)
1637+826	NGC 6251	G	0.024	$3.5 \pm 0.3$	$3.65 \pm 0.08$	$1.9 \pm 0.3$	Kovalev et al. (2020)
1807+698	3C 371	B	0.051	$1.0 \pm 0.2^1$	$1.22 \pm 0.07$	$1.5 \pm 0.3$	Kovalev et al. (2020)
1957+405	Cygnus A	G	0.056	$1.72 \pm 0.09$	$3.9 \pm 0.8$	$\sim 2$ ; $\sim 5$	Boccardi et al. (2016), Krichbaum et al. (1998)
2013+370	TXS 2013+370	Q	0.859	$\sim 0.6^1$	$\sim 0.5^1$	$\sim 0.5$	Traianou et al. (2020)
2200+420	BL Lac	B	0.069	$2.43 \pm 0.05$	$1.37 \pm 0.02$	$2.5 \pm 0.1$	Kovalev et al. (2020)

We confirm 9(16) cases.

The jet geometry transition is accompanied by break in  $T_b$ !

$T_b$  and  $R(r)$  behave differently.

The shape of profiles doesn't depend on existence of a stationary feature.



# LOS scenario

The emission pattern located closer to the observer relative to the jet axis, e.g. the near side, will make smaller angle to the LOS than the far side, so their Doppler factors will be different.

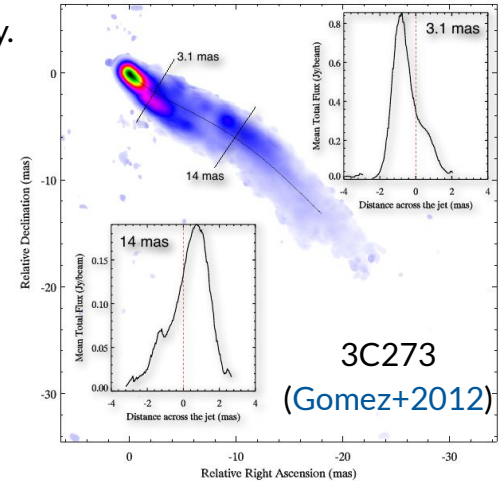
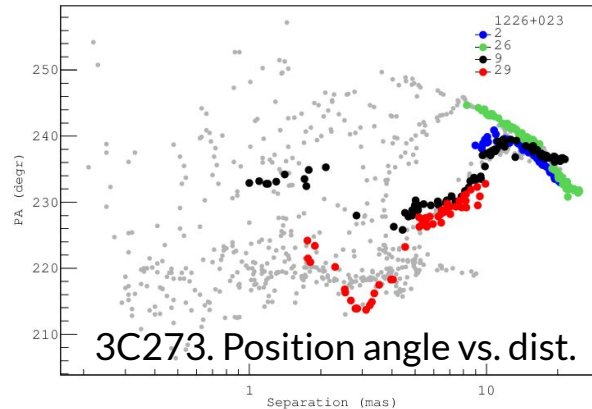
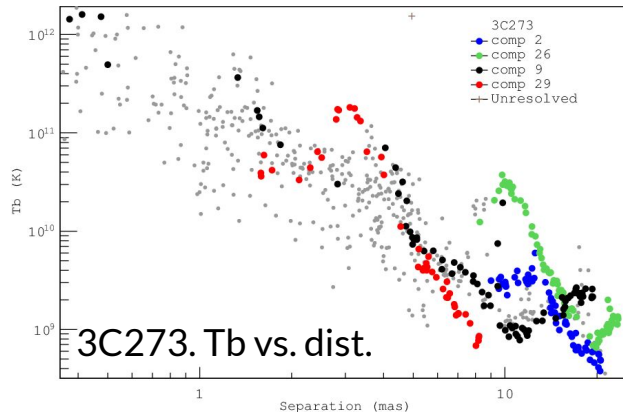
**Non-radial motion:** components that have significant non-radial motions, i.e. which trajectories do not extrapolate back to the jet base, that indicates directional changes of the jet features (Lister et al. 2009; Homan et al. 2015):

198 jets show non-radial motion; 165 (83%) out of these show broken profiles. 66 jets with the break have no non-radial counterparts

**Helical jets/structures:**

There are at least 38 jets with clear zigzag pattern, in 16 of them transverse Faraday RM gradients or evidences for helical MF are observed.

Breaks are also observed for the jets with the transverse emission stratification/asymmetry.



# Stationary features / shocks

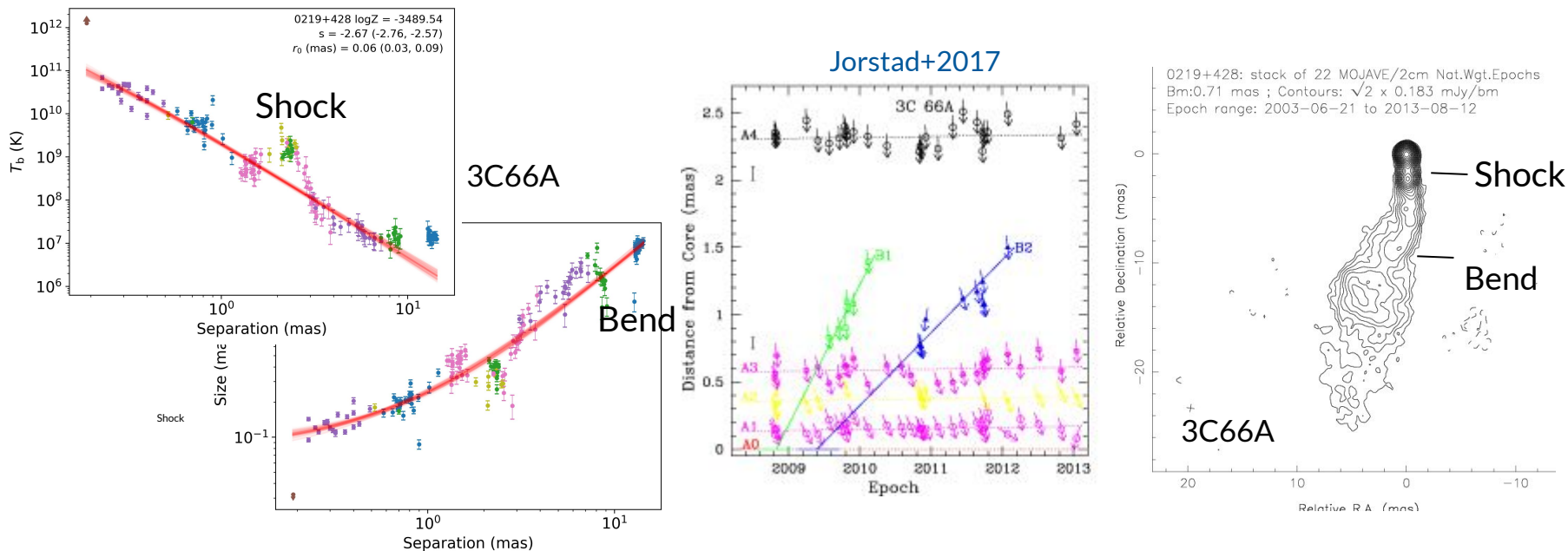
Individual studies suggests association of broken Tb(r) & R(r) profiles with shocks in the jet:

CTA 102 (Fromm+2012), 3C66A (Bottcher+2013), 3C111 (Beuchert+2019).

54 features in 42 sources show slow pattern speeds ( $\beta_{app} < 0.2c$ ) based on kinematics (Lister+2019).

24 out of these 42 sources show broken profiles.

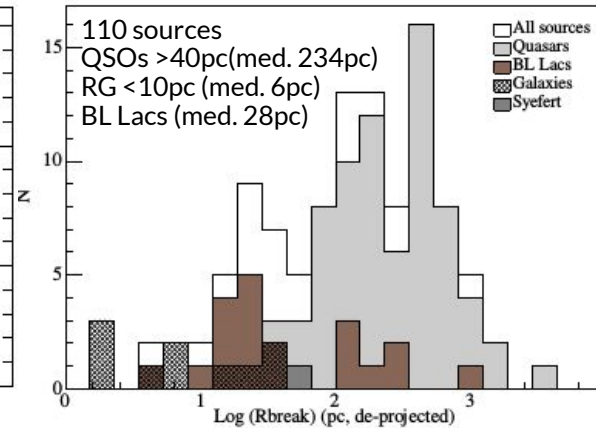
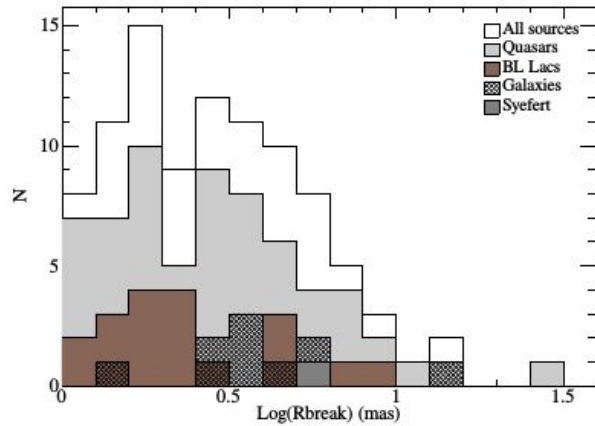
In 18 of 24 jets the break coincides with the median position of a stationary component.



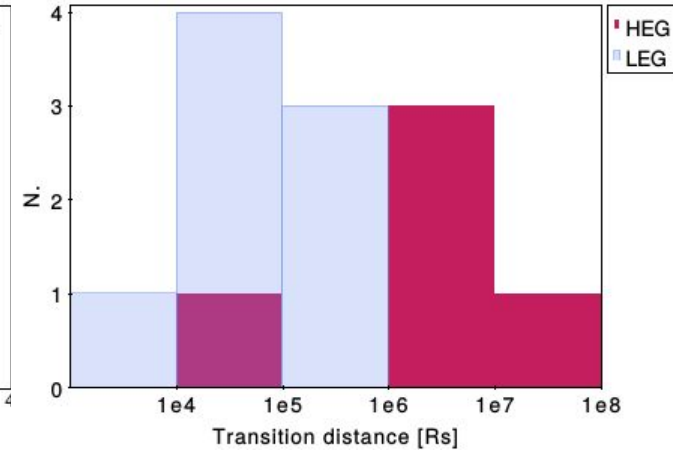
# Distance of the break position

Distribution of  $r_{\text{break}}$  for different classes (141 sources)

Estimates of viewing angles or maximum  $\beta_{\text{app}}$  are used (Hovatta+2012; Lister+2019)



Hervett+2018, Boccardi+2021



The jet instabilities (recollimation) in quasars are located farther than in BL Lacs and galaxies. This is consistent with the models of jet launching that depends on the main accretion mode: collimation and acceleration is longer in more powerful sources.

Need to be careful regarding selection criteria, as quasars as observed at further distances.



# Physical parameters along jets

Using assumption of power-law dependence of physical parameters along jets and that jet features are optically thin blobs:

$$T_b(r) \propto N(r)B(r)^{1-\alpha}R(r)\delta(r)^{3-\alpha},$$

$$B \propto r^b, B \propto R(r)^{b'},$$

$$N \propto r^n, N \propto R(r)^{n'},$$

$$R \propto r^d,$$

$$\delta \propto r^p, \delta \propto R^{p'}.$$

Therefore,

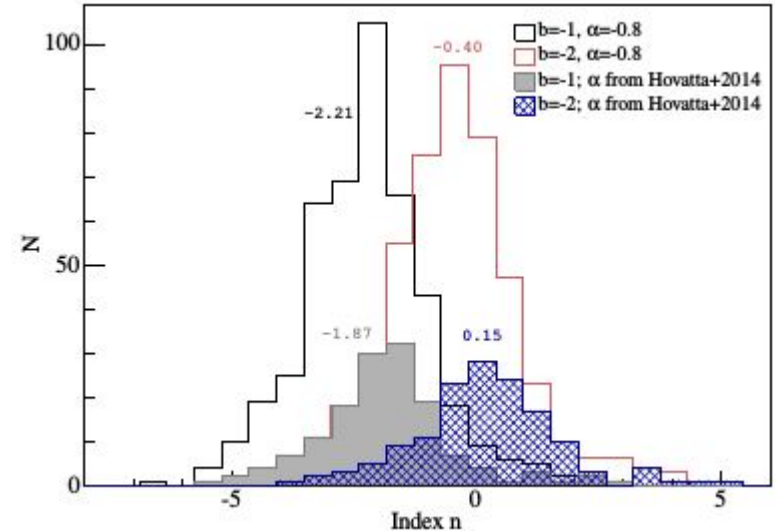
$$T_b(r) \propto r^s,$$

$$T_b(R) \propto R^{s'},$$

$$s = n + b(1 - \alpha) + d + p(3 - \alpha),$$

$$s' = n' + b'(1 - \alpha) + 1 + p'(3 - \alpha).$$

$N(\gamma) \propto \gamma^{-\epsilon}$  that results in the spectral index  $\alpha = (1 - \epsilon)/2$ , defined as  $S \propto \nu^\alpha$ , where  $S$  is the flux density observed at frequency  $\nu$ .



**b=-1; n=-2, p=0, alpha=-0.8:**

- toroidal MF dominates (models of shocked jets/Poynting);
- equipartition between Ne and B energies;
- mass conservation (n=-2d).

# Shock-in-jet model (Marscher&Gear 1985)

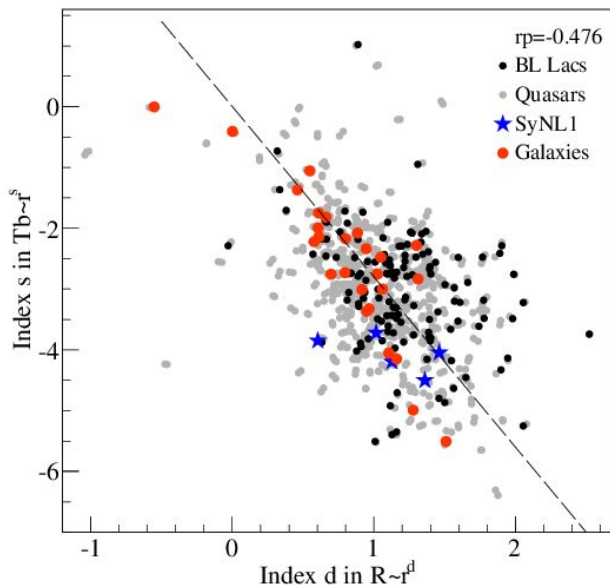
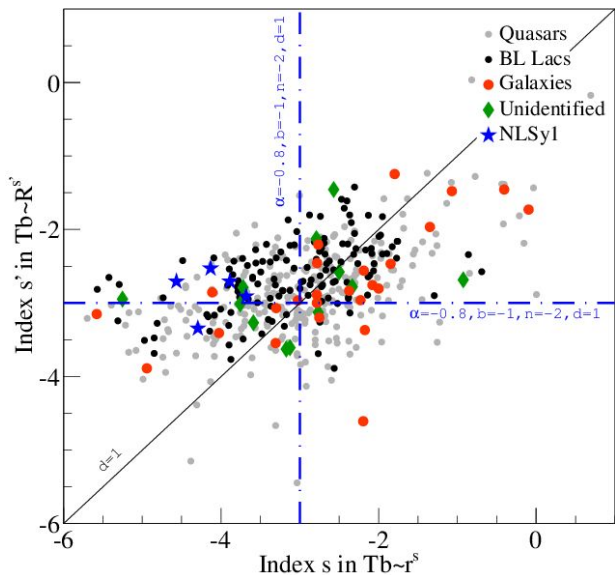
Assume that components are moving shocks. Adiabatic losses due to expansion are the main mechanism. Compton and synchrotron losses can be neglected.

$$T_{b,\text{jet}}(R) \propto R^{s'_{\text{ad}}}; s'_{\text{ad}} = -[2(2\epsilon + 1) - 3b(\epsilon + 1) - 3p(\epsilon + 3)]/6;$$

Median  $s/s' \equiv d = 1.05$ . From  $R(r)$  fits median  $d = 1.01$ .

$$T_{b,\text{jet}}(r) \propto r^{s_{\text{ad}}}, s_{\text{ad}} = d s'_{\text{ad}}.$$

The estimated  $s$  and  $s'$  values are consistent with adiabatic loss phase if moderate variability in Doppler factor is presented ( $\delta \sim r^{0.4}$ ).



$$s = d + n + b(1 - a)$$

Assuming mass conservation:

$$(n = -2d), s = b(1 - \alpha) - d.$$

Conservation of magnetic flux implies

$$b = -d, \text{ therefore } s = d(\alpha - 2).$$

# Summary

---

1.  $T_b(r)$  and  $R(r)$  catch various inhomogeneities in the AGN jets.
2. Because of 1, unfortunately, a number of phenomena can explain observed profiles, which is difficult to distinguish. This requires per-source analysis.
3. The jet shape recollimation region is accompanied by a broken  $T_b(r)$  profile.
4. Most of variations can be explained by change in PA of the emitting region relative to the LOS (like bends, shocks, interaction with external medium, helical jets, helical structures, helical magnetic field, jet rotation).
5. Distribution of the break distances is different for different AGN classes: in galaxies and BL Lacs are closer to center, in quasars farther.
6. Slopes of  $T_b(r)$  and  $R(r)$  distributions are consistent with the canonical scenario of equipartition ( $N \sim r^{-2}$ ); predominantly toroidal magnetic field ( $B \sim r^{-1}$ ); and mass conservation ( $N \sim R^{-2}$ ).
7. Gradients of  $T_b$ -size and  $T_b$ -distance are consistent with the shock-in-jet model with the adiabatic expansion under assumption that Doppler factor varies along the jet.